DALTON
FULL PAPER

The role of π–π stacking interactions in stabilising trigonal planar copper(I) in Cu(BF_4)–2,9-dimethyl-1,10-phenanthroline–nitrile systems†

Alexander J. Blake, Peter Hubberstey,* Wan-Sheung Li, Daniel J. Quinlan, Claire E. Russell and Claire L. Sampson

School of Chemistry, Nottingham University, Nottingham, UK NG7 2RD.
E-mail: peter.hubberstey@nottingham.ac.uk

Received 20th August 1999, Accepted 12th October 1999

Crystallisation from MeCN solutions containing copper(I) tetrafluoroborate, 2,9-dimethyl-1,10-phenanthroline (dmp) and either 2-cyanoguanidine (cnge) or one of its substituted derivatives, 2-cyano-*N*,*N*′-dimethylguanidine (dmcnge) and 2-cyanoimino-4,6-pyrimidine (cidmp), by Et_2O vapour diffusion methods yielded [Cu(dmp)(nitrile)][BF_4]·*x*MeCN (nitrile = cnge, *x* = 1 **2**; dmcnge, *x* = 0; or cidmp, *x* = 0). In the absence of an added nitrile [Cu(dmp)(NCMe)][BF_4] **3** formed. Crystallisation from CH_2Cl_2 solutions containing copper(I) tetrafluoroborate, dmp and cnge by Et_2O vapour diffusion methods yielded [Cu(dmp)(cnge)][BF_4]·0.5Et_2O **1**. Structural studies of **1**, **2** and **3** have established that the [Cu(dmp)(nitrile)]$^+$ cations are three-co-ordinate trigonal planar (Y-shaped) species with bidentate dmp and monodentate nitrile ligands. The MeCN molecule in **2** is hydrogen bonded to the cnge ligand in a position adjacent to the copper(I) atom. When **1**, **2** and **3** are combined with a tetrahedral copper(I) species co-ordinated by a bidentate ligand, cnge and MeCN, they represent stages in a crystallographic sequence depicting associative substitution at trigonal planar copper(I). In solution an equilibrium [K_e = 3.9(6) at 298 K] exists between [Cu(NCMe)$_4$]$^+$, [Cu(dmp)(nitrile)$_x$]$^+$ (*x* = 1 or 2) and [Cu(dmp)$_2$]$^+$ cations, indicating that the stability of the [Cu(dmp)(nitrile)]$^+$ cations in the solid phase must be due to intermolecular packing interactions. For all three structurally characterised complexes, π–π (face-to-face) stacking interactions between co-ordinated dmp molecules generate an efficient parallel packing system thus promoting the trigonal planar copper(I) co-ordination geometry.

The active centres of deoxyhaemocyanins comprise two copper(I) atoms, trigonally co-ordinated by three histidine ligands and separated by *ca*. 4 Å.[1] Binding of dioxygen occurs in a μ-η^2,η^2 fashion and results in a reduction of the copper–copper separation to *ca*. 3.6 Å.[2] Following our success in stabilising three-co-ordinate copper(I) with 2-cyanoguanidine (cnge) [3–6] and Munakata's report of the three-co-ordinate copper(I) cation [Cu(dmp)(NCMe)]$^+$ (dmp = 2,9-dimethyl-1,10-phenanthroline),[7] we targeted, as a model of deoxyhaemocyanins, a dinuclear complex comprising two three-co-ordinate copper(I) centres bridged by a bis(bidentate) ligand and terminally co-ordinated by cnge [Scheme 1(a)]. Despite diverse attempts using a variety of substituted 3,6-bis(pyrazol-1-yl)-pyridazines [Scheme 1(a)] as bis(bidentate) ligands, the only products were four-co-ordinate tetrahedral copper(I) species, the trinuclear [Cu{(μ-ppdBu)Cu(cnge)(NCMe)}$_2$]$^{3+}$ [Scheme 2(a)][8] and the tetranuclear [Cu$_4$(μ-ppd)$_4$]$^{4+}$ [Scheme 2(b)].[9] To identify reasons for this lack of success, three-co-ordinate analogues of Munakata's complex,[7] based on dmp and cnge ([Cu(dmp)(cnge)]$^+$; Scheme 1(b)) were targeted. Here, we describe the synthesis, solution dynamics and solid state structures of three trigonal planar copper(I) complexes with co-ordinated dmp and either cnge or MeCN, [Cu(dmp)(cnge)][BF_4]·0.5Et_2O **1**, [Cu(dmp)(cnge)][BF_4]·MeCN **2** and [Cu(dmp)(NCMe)][BF_4] **3**. Interestingly, when **1**, **2** and **3** are combined with the structure of a tetrahedral copper(I) centre co-ordinated by a dmp analogue, cnge and MeCN (*e.g.*, one of the terminal copper atoms of the trinuclear cation, [Cu{(μ-ppdBu)Cu(cnge)(NCMe)}$_2$]$^{3+}$ **4**)[8] the four structures form a sequence depicting associative substitution of cnge by MeCN.

The factors controlling the stabilisation of three-co-ordinate copper(I)[10] are not fully understood, despite several preliminary theoretical studies.[5,11] Although the ability of sterically demanding (bulky monodentate[12]) or structurally constraining (multidentate[13] and macrocyclic[14]) ligands to generate trigonal planar copper(I) is readily appreciated, that of sterically non-demanding (halides,[15] cyanide,[16] 2-cyanoguanidine,[3–6] phenanthrolines,[7] *etc.*) ligands is less so. We believe that intermolecular

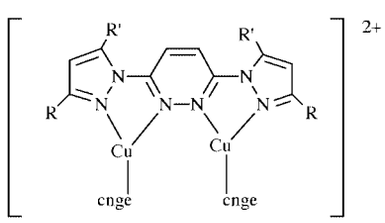

(a)

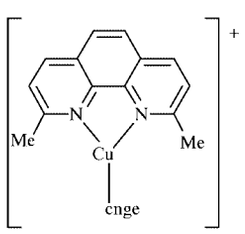

(b)

R = R′ = H: 3,6-bis(pyrazol-1-yl)pyridazine (ppd). R = R′ = Me: 3,6-bis(3,5-dimethylpyrazol-1-yl)pyridazine (ppdMe). R = ^{t}Bu, R′ = H: 3,6-bis(3-*tert*-butylpyrazol-1-yl)pyridazine (ppdBu).

Scheme 1 Target molecules for (a) the copper(I) tetrafluoroborate–2-cyanoguanidine–3,6-bis(pyrazol-1-yl)pyridazine and (b) the copper(I) tetrafluoroborate–2-cyanoguanidine–2,9-dimethyl-1,10-phenanthroline systems.

† *Supplementary data available*: rotatable 3-D crystal structure diagram in CHIME format. See http://www.rsc.org/suppdata/dt/1999/4261/

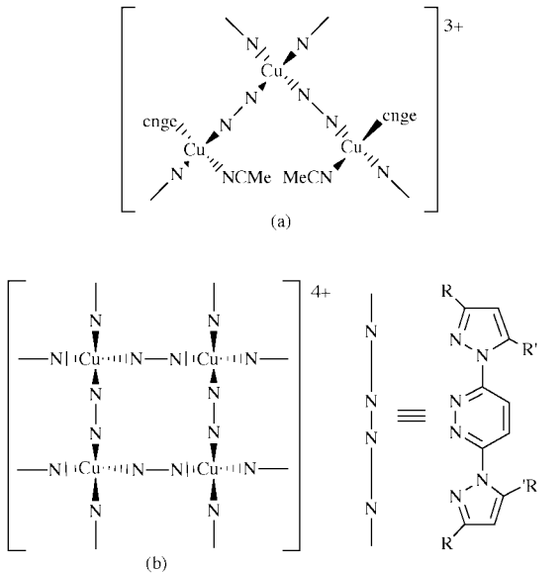

Scheme 2 Products formed in the copper(I) tetrafluoroborate–2-cyanoguanidine–3,6-bis(pyrazol-1-yl)pyridazine systems: (a) trinuclear complexes with ppdBu and (b) tetranuclear complexes with ppd or ppdMe.

packing interactions are more important than previously thought and have recently argued[17,18] that the formation of three-co-ordinate copper(I) in some $Cu(BF_4)$–cnge complexes is a consequence of the parallel packing of two-dimensional sheets constructed by N–H · · · F contacts. In this paper we propose that π–π (face-to-face) stacking interactions between dmp ligands result in the parallel packing of $[Cu(dmp)L]^+$ (L = cnge or NCMe) cations, thus promoting three-co-ordinate copper(I) cation geometry.

Results and discussion

Diverse cations, $[Cu(dmp)_2]^+$, $[Cu(NCMe)_4]^+$, $[Cu(dmp)(cnge)]^+$ and $[Cu(dmp)(NCMe)]^+$, form on crystallisation from acetonitrile or dichloromethane solutions containing copper(I) tetrafluoroborate, dmp and cnge. The compounds, obtained by solvent–solvent vapour diffusion methods, were initially identified by elemental analysis (C, H, N) and IR spectroscopy and subsequently characterised by single crystal X-ray diffraction methods. Oscillation and Weissenberg photographs confirmed the formation of the starting material, $[Cu(NCMe)_4][BF_4]$ **5** (isostructural with $[Cu(NCMe)_4][ClO_4]$[19]) and of the ether solvate of $[Cu(dmp)_2][BF_4]$ **6**.[18] They also indicated the separate identities of the mixed ligand compounds $[Cu(dmp)(cnge)][BF_4]\cdot 0.5Et_2O$ **1** (isolated from CH_2Cl_2), $[Cu(dmp)(cnge)][BF_4]\cdot MeCN$ **2** (isolated from MeCN) and $[Cu(dmp)(NCMe)][BF_4]$ **3**, the structures of which were determined from diffraction data. Although $[Cu(dmp)(NCMe)][BF_4]$ is isostructural with the corresponding perchlorate,[7] we considered it pertinent to determine its structure in view of the sequence depicting associative substitution of cnge by MeCN.

^{1}H NMR studies of acetonitrile solutions containing copper(I) tetrafluoroborate, dmp and cnge and of complexes **1**–**3**, **5** and **6** were consistent with the presence of $[Cu(dmp)_2]^+$, $[Cu(dmp)(NCMe)_x]^+$ ($x = 1$ or 2) and $[Cu(NCMe)_4]^+$ suggesting that $[Cu(dmp)(cnge)]^+$ is formed during the crystallisation process.

Analogous complexes, $[Cu(dmp)(dmcnge)][BF_4]$ **7** and $[Cu(dmp)(cidmp)][BF_4]$ **8**, containing substituted 2-cyanoguanidines with modified hydrogen bonding potential, 2-cyano-*N*,*N*-dimethylguanidine (dmcnge) and 2-cyanoimino-4,6-dimethylpyrimidine (cidmp), were also synthesized and identified. Unfortunately, neither formed crystals suitable for

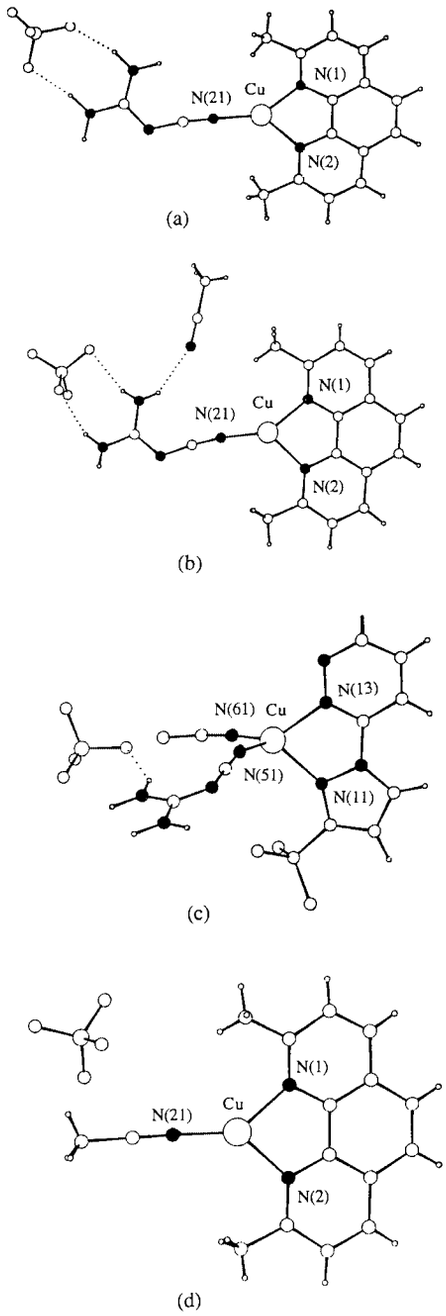

Fig. 1 The molecular structures of (a) $[Cu(dmp)(cnge)][BF_4]\cdot 0.5Et_2O$, (b) $[Cu(dmp)(cnge)][BF_4]\cdot MeCN$, (c) one of the terminal copper(I) centres in $[Cu\{(\mu\text{-ppdBu})Cu(cnge)(NCMe)\}][BF_4]_3\cdot MeCN$ and (d) $[Cu(dmp)(NCMe)][BF_4]$ depicting the associative substitution of 2-cyanoguanidine by acetonitrile at trigonal planar copper(I). [In the ligands, open circles represent carbon atoms and filled circles nitrogen atoms.]

structural analysis. Nonetheless, proof of ligand co-ordination was obtained from IR spectral data. In particular, perturbation of the ν_{asym}(NCN) absorption of cnge and its substituted derivatives confirms co-ordination. For cnge, Fermi resonance gives rise to a "doublet" at 2209/2165 cm^{-1}.[20] The shift to 2206/2162 cm^{-1} for **1** and **2** is typical of cnge co-ordinated to copper(I).[3–6,21] For free dmcnge and cidmp a single band is observed at 2168 and 2208 cm^{-1}, respectively. On co-ordination in **7** and **8** this band moves marginally to lower energy at 2163 and 2203 cm^{-1}, respectively.

Crystal and molecular structures of complexes 1, 2 and 3

The molecular structures of complexes **1**, **2** and **3** are shown, together with that of one of the terminal copper centres in $[Cu\{(\mu\text{-ppdBu})Cu(cnge)(NCMe)\}_2]^{3+}$ **4**,[8] in Fig. 1. Selected

Table 1 Interatomic distances (Å) and angles (°) for [Cu(dmp)(cnge)][BF_4]·0.5Et_2O **1**, [Cu(dmp)(cnge)][BF_4]·MeCN **2**, [Cu(dmp)(NCMe)][BF_4] **3**, [Cu{(μ-ppdBu)Cu(cnge)(NCMe)}$_2$][BF_4]$_3$·MeCN **4**[a] and [Cu(cnge)(NCMe)(μ-pyz)][BF_4]·0.5pyz **10**[b]

				4[a]		
Complex	**1**	**2**	**3**	Cu(1)	Cu(3)	**10**[b]
Cu–N (1-dmp)	1.999(6)	2.014(4)	2.019(2)	2.103	2.158	2.100
Cu–N (2-dmp)	2.036(6)	2.054(4)	2.034(2)	2.042	2.065	2.076
Cu–N (cnge)	1.818(6)	1.851(3)	—	1.941	1.928	1.965
Cu–N (NCMe)	—	—	1.856(2)	1.949	1.934	1.928
N (1-dmp)–Cu–N (2-dmp)	82.4(3)	82.8(1)	83.17(6)	77.8	77.7	112.3
N (1-dmp)–Cu–N (cnge)	143.5(3)	147.1(2)	—	114.8	104.1	105.5
N (2-dmp)–Cu–N (cnge)	133.9(3)	130.2(2)	—	114.5	108.1	109.1
N (1-dmp)–Cu–N (NCMe)	—	—	140.79(7)	114.3	117.9	105.7
N (2-dmp)–Cu–N (NCMe)	—	—	135.88(7)	127.5	123.6	107.7
N (cnge)–Cu–N (NCMe)	—	—	—	105.8	117.7	116.7
Cu–N (cnge)–C (cnge)	177.8(8)	172.2(4)	—	161.7	169.8	172.6
Cu–N (NCMe)–C (NCMe)	—	—	174.1(2)	168.7	171.1	169.7

[a] For complex **4**, N(1-dmp) is a pyrazole nitrogen and N(2-dmp) is a pyridazine nitrogen of the tetradentate ligand. [b] For complex **10**, N(1-dmp) and N(2-dmp) are pyrazine nitrogens.

Table 2 Hydrogen bonding contacts in complexes **1**, **2**, **4** and **10**

Interaction N–H···X	Symmetry of X	N–H/Å	N–X/Å	H···X/Å	N–H–X/°
[Cu(dmp)(cnge)][BF_4]·0.5Et_2O **1**					
N(12)–H(231)···F(14)	$(1-x, y, 1.5-z)$	1.00	2.913(9)	1.99	153
N(23)–H(232)···F(12)	(x, y, z)	1.00	2.920(8)	1.94	164
N(24)–H(241)···F(13)	(x, y, z)	1.00	2.920(8)	1.93	169
N(24)–H(242)···N(22)	$(1-x, -y, 1-z)$	1.00	2.983(10)	1.99	175
[Cu(dmp)(cnge)][BF_4]·MeCN **2**					
N(23)–H(231)···N(31)	(x, y, z)	0.82(6)	2.972(6)	2.27(6)	145(6)
N(23)–H(232)···F(12)	(x, y, z)	0.79(6)	3.214(5)	2.46(7)	160(6)
N(23)–H(232)···F(13)	(x, y, z)	0.79(6)	3.178(6)	2.49(7)	146(6)
N(24)–H(241)···F(13)	(x, y, z)	0.86(7)	2.926(6)	2.11(8)	159(7)
N(24)–H(242)···F(14)	$(x, 0.5-y, -0.5+z)$	0.77(5)	2.903(6)	2.15(5)	166(5)
[Cu{(μ-ppdBu)Cu(cnge)(NCMe)}$_2$][BF_4]$_3$·MeCN **4**					
N(53)–H(531)···F(12)	(x, y, z)	1.00	2.96(3)	2.07	147
N(53)–H(532)···F(33)	$(1-x, -y, 1-z)$	1.00	3.05(2)	2.18	144
N(54)–H(541)···F(33)	$(1-x, -y, 1-z)$	1.00	2.96(2)	2.04	151
N(54)–H(542)···F(31)	$(x, y, 1+z)$	1.00	2.96(2)	2.03	154
N(73)–H(731)···N(52)	(x, y, z)	1.00	3.15(3)	2.42	130
N(73)–H(732)···F(34)	$(x, y, 1+z)$	1.00	3.13(2)	2.35	134
N(74)–H(741)···N(91)	$(x, -1+y, 1+z)$	1.00	3.11(2)	2.16	159
N(74)–H(742)···F(32)	$(2-x, -y, 1-z)$	1.00	3.13(2)	2.18	158
[Cu(cnge)(NCMe)(μ-pyz)][BF_4]·0.5pyz **10**					
N(23)–H(231)···N(11)	(x, y, z)	0.99	2.91(2)	1.96	162
N(23)–H(232)···F(12)	(x, y, z)	1.02	2.88(2)	1.90	161
N(24)–H(241)···F(13)	(x, y, z)	1.03	3.14(2)	2.15	160
N(24)–H(242)···F(11)	$(x, -0.5-y, -0.5+z)$	0.97	3.03(2)	2.31	130

interatomic distances and angles are collected in Table 1. Hydrogen-bonding parameters for complexes **1** and **2** are summarised in Table 2. All three complexes comprise [Cu(dmp)(nitrile)]$^+$ cations and unco-ordinated BF_4^- anions; **1** and **2** also contain Et_2O and MeCN solvate molecules, respectively. The [Cu(dmp)(nitrile)]$^+$ cations adopt similar trigonal planar geometries [Fig. 1(a), (b), (d)] with no internal symmetry elements (*e.g.*, C_2 axes or σ_v planes). Although the co-ordination of the bidentate dmp ligands differs little (Table 1) that of the nitriles differs in its location relative to the pseudo twofold symmetry axis of the chelating dmp ligand. This difference can be quantified by the difference in the angle at the copper centre between the ligating nitrogen of the nitrile and the midpoint of the vector joining the two dmp nitrogens, which increases from 4.91 (**3**) through 9.6 (**1**) to 16.9° (**2**). The Cu–N (dmp) distances [average: 2.026(19) Å (Table 1)] are considerably longer than the Cu–N (nitrile) distances [average: 1.842(21) Å (Table 1)]. The difference (0.184 Å) can be compared to that in other three-co-ordinate *N*-ligated copper(I) complexes; it is similar to those (0.215, 0.191 Å) in [{Cu(cnge)$_2$}$_2$(μ-4,4′-bipy)$_2$]$^{2+}$ (4,4′-bipy = 4,4′-bipyridine)[3] but greater than that (0.089 Å) in [{Cu(cnge)}$_2$(μ-pydz)$_2$]$^{2+}$ (pydz = pyridazine).[6] Despite being influenced by intermolecular packing interactions, it is clearly based on the differing N(sp^2) and N(sp) radii.

The extreme distortion in complex **2** is undoubtedly due to the presence of the MeCN molecule hydrogen bonded to the co-ordinated cnge [Fig. 1(b); Table 2]. This structural motif is not unique; it also occurs in [{Cu(cnge)$_2$}(μ-4,4′-bipy)][BF_4]$_2$·MeCN **9**.[3] The similarity of the two arrangements is clear from their comparison in Fig. 2 and the structural param-

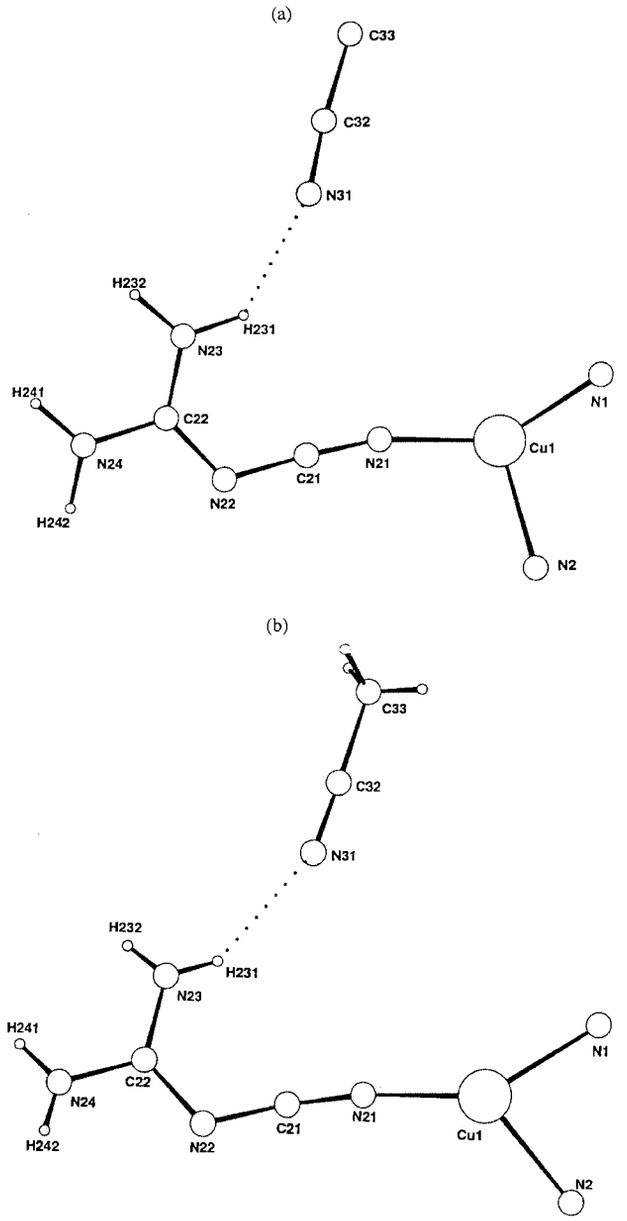

Fig. 2 Comparison of the molecular arrangements of the inner and outer co-ordination spheres of the copper(I) centres in (a) [{Cu(cnge)$_2$}$_2$(μ-4,4′-bipy)][BF$_4$]$_2$·MeCN and (b) [Cu(dmp)(cnge)][BF$_4$]·MeCN.

eters collated in Table 3. The only difference lies in the N–Cu–N angles remote from the acetonitrile molecule. Similar in **9** [N(1)–Cu(1)–N(2) 107.6, N(2)–Cu(1)–N(21) 106.9°], they differ in **2** [N(1)–Cu(1)–N(2) 82.8, N(2)–Cu(1)–N(21) 130.0°], owing to the structural demands (bite angle) of the chelating dmp ligand.

The ether molecules in complex **1** are sited in cavities centered at (0, 0.386, 1/4); they have no influence on the copper(I) co-ordination geometry.

In complexes **1** and **2** the BF_4^- anions are held in position by the double N–H···F hydrogen bonding contacts [Fig. 1(a), 1(b), Table 2] typical of cnge–BF_4^- systems.[22] In complex **3**, however, there is no potential for hydrogen bonding and the BF_4^- anion is located in a hydrophobic cavity.

Stabilisation of three-co-ordinate copper(I)

We have recently argued[17,18] that the formation of three co-ordinate copper(I) in $CuBF_4$–cnge complexes[3–6] may not be an intrinsic property of the complex but may arise as a consequence of the parallel packing of two-dimensional sheets, the formation of which depends on extensive N–H···F hydrogen-bonding networks. Although similar N–H···F contacts are seen in **1** and **2** [Fig. 1(a), 1(b)], this argument is inapplicable for three-co-ordinate [Cu(dmp)(nitrile)]$^+$ cations as they are formed by both cnge and MeCN. Nonetheless, we still believe that the stabilisation of trigonal planar copper(I) results from intermolecular packing interactions, in this case π–π stacking between dmp molecules. The packing diagrams for **1**, **2** and **3** are shown in Fig. 3. For all three complexes adjacent dmp planes are virtually parallel as evidenced by the extremely small dihedral angles between the normals to their least squares planes (**1** 0.9; **2** 0.9; **3** 2.6°) and the limited range in the perpendicular separations between atoms in one dmp molecule and the least squares plane of the other (**1** 0.13; **2** 0.17; **3** 0.15 Å). The separations between planes (**1** 3.40–3.53; **2** 3.23–3.40; **3** 3.18–3.43 Å) are typical of π–π stacked systems [*cf.* graphite 3.354 Å]. Diagrams showing the overlap between parallel cations are shown in Fig. 4. Their relative orientation is inconsistent (Fig. 4); in **1** they face opposite directions, in **2** they face the same direction and in **3** they adopt a skewed arrangement, observations which infer there is no preferred packing arrangement. The significance of π–π stacking interactions in structure determination is well established.[18,23] In these crystals they enforce parallel coplanar constructions thereby stabilising trigonal planar copper(I) co-ordination geometries. With [Cu(dmp)L]$^+$ cations such arrangements can only be generated with nitriles as the co-ligand. With bulkier ligands, *e.g.* pyridines, there is insufficient room for coplanarity of the two ligands. The orthogonal ligands destroy the efficient packing arrangements and four-co-ordinate tetrahedral copper(I) results (*e.g.*, [{Cu(dmp)(NCMe)}$_2$(μ-diimine)]$^{2+}$ or {[Cu(dmp)-(μ-diimine)]$^{2+}$}$_n$.[18]

Table 3 Interatomic distances (Å) and angles (°) for the "incipient" co-ordination of MeCN in [Cu(dmp)(cnge)][BF$_4$]·MeCN **2** and [{Cu(cnge)$_2$}$_2$(μ-4,4′-bipy)][BF$_4$]$_2$·MeCN **9**

Complex	**2**	**9**
N(23)···N(31)	2.972	2.948
N(23)–H(231)	0.82	1.00
H(231)···N(31)	2.27	2.14
N(23)–H(231)···N(31)	145	137
N(31)···Cu(1)	4.69	4.92
C(32)–N(31)···Cu(1)	125.6	128.3
C(32)–N(31)···H(231)	157.1	157.1
Cu(1)···N(31)···H(231)	73.8	65.4
N(1)–Cu(1)···N(31)	93.2	94.3
N(31)···Cu(1)–N(21)	54.7	51.3
N(21)–Cu(1)–N(1)	147.1	145.5
N(21)–Cu(1)–N(2)	130.0	106.9
N(2)–Cu(1)–N(1)	82.8	107.6

Associative substitution of cnge by MeCN

Complex **2** forms part of the mechanistic pathway between **1** and **3**. The hydrogen bonded MeCN molecule is ideally located to facilitate the formation of a four-co-ordinate intermediate. The required intermediate, [Cu(dmp)(cnge)(NCMe)]$^+$, is inaccessible in the solid state owing to the stabilisation of three-co-ordinate copper(I) in **1**, **2** and **3**. A search of the literature revealed two cations containing four-co-ordinate copper(I) with co-ordinated cnge and MeCN, [Cu{(μ-ppdBu)[Cu(cnge)-(NCMe)]}$_2$]$^{3+}$ **4**[8] and {[Cu(cnge)(NCMe)(μ-pyz)]$^+$}$_\infty$ **10** (pyz = pyrazine).[21] The terminal copper centres in **4** are more appropriate as they are co-ordinated by a chelating bidentate fragment of a bis(bidentate) ligand as well as cnge and MeCN molecules. In **10** the copper centre is co-ordinated by two pyz molecules, which bridge to adjacent copper atoms to form a zigzag chain, as well as the cnge and MeCN ligands. The co-ordination sphere of one of the terminal copper centres in **4** is

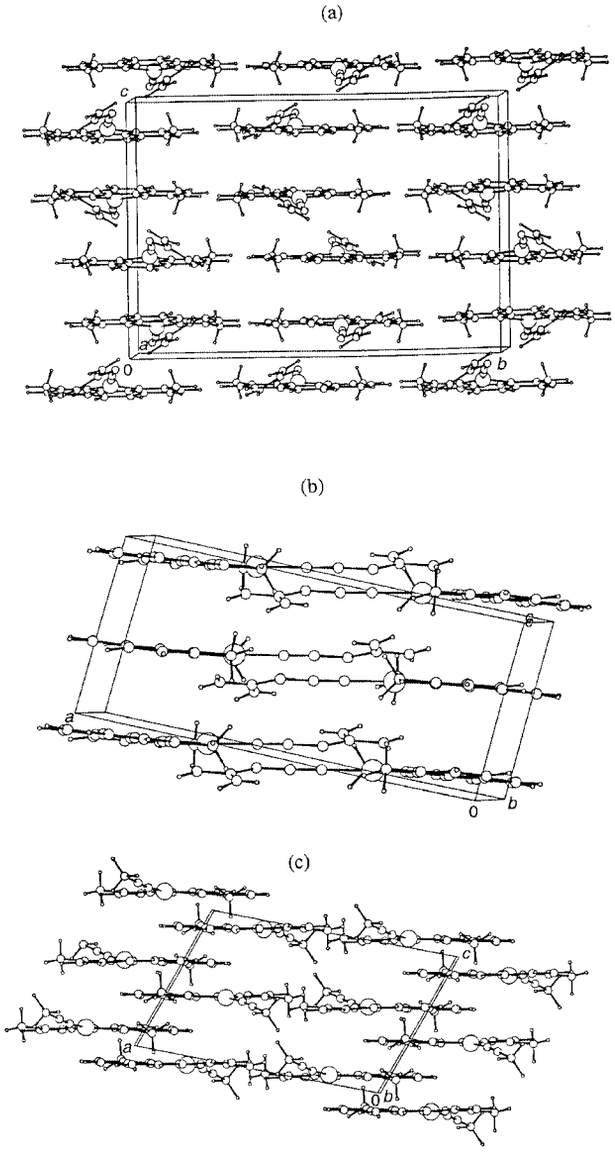

Fig. 3 Packing diagrams showing the parallel stacking of the cations of (a) $[Cu(dmp)(cnge)][BF_4]\cdot 0.5Et_2O$, (b) $[Cu(dmp)(cnge)][BF_4]\cdot MeCN$ and (c) $[Cu(dmp)(NCMe)][BF_4]$.

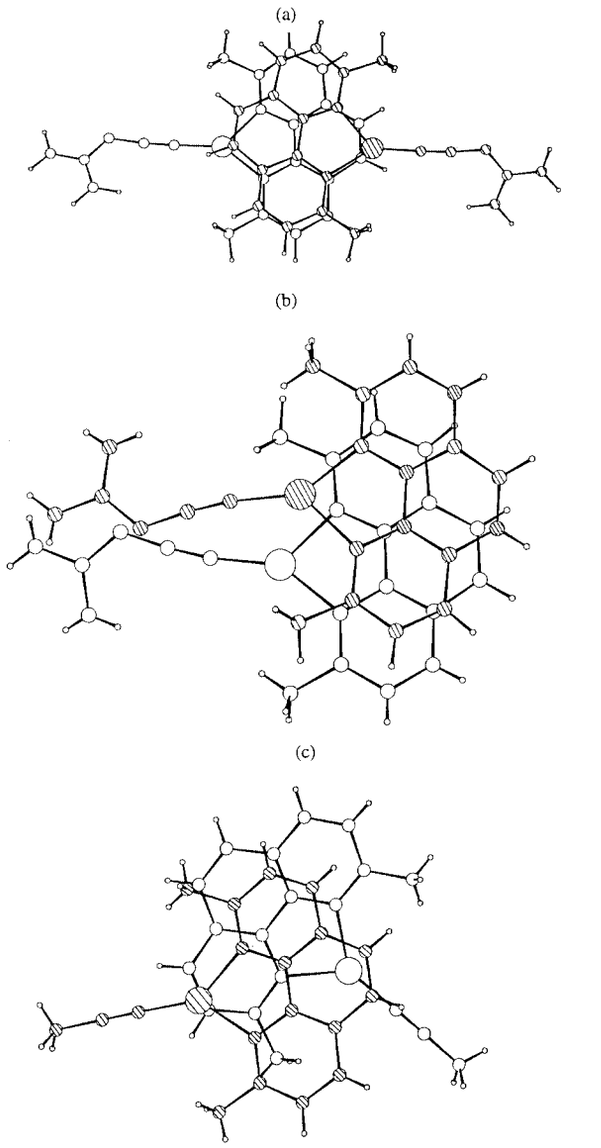

Fig. 4 Projections of the cations of (a) $[Cu(dmp)(cnge)][BF_4]\cdot 0.5Et_2O$, (b) $[Cu(dmp)(cnge)][BF_4]\cdot MeCN$ and (c) $[Cu(dmp)(NCMe)][BF_4]$ perpendicular to the planar copper(I) co-ordination geometries showing the differing overlap arrangements of the 2,9-dimethyl-1,10-phenanthroline ligands. [Open and shaded circles represent atoms in parallel pairs of cations.]

shown in Fig. 1(c) to complete the mechanistic sequence [Fig. 1(a)–(d)]. Selected structural parameters from the copper(I) co-ordination geometries and the N–H · · · F contacts in **4** and **10** are included in Tables 1 and 2, respectively. Expansion of the co-ordination geometry is accompanied not only by a decrease in the non-chelating bond angles, but also by an increase in copper–nitrogen distances [average Cu–N (nitrile) 1.842(21) to 1.938(15); average Cu–N (bidentate chelate) 2.026(19) to 2.092(36) Å (Table 1)]. The four structures form a sequence depicting associative substitution of 2-cyanoguanidine by acetonitrile.

Acetonitrile solution dynamics of $[Cu(dmp)(nitrile)]^+$ cations

The ^1H NMR room temperature spectra of complexes **1**, **2** and **3** in CD_3CN are identical. Variable temperature (233–288 K) spectra for **3** are compared with the 298 K spectrum of $[Cu(dmp)_2][BF_4]$ **6** in Fig. 5. They are consistent with the presence of $[Cu(dmp)_2]^+$ and $[Cu(dmp)(NCMe)_x]^+$ in the equilibrium (1). The $[Cu(dmp)_2]^+$ resonances are sharp and

$$2[Cu(dmp)(NCMe)_x]^+ \underset{K_e}{\overset{MeCN}{\rightleftharpoons}} [Cu(dmp)_2]^+ + [Cu(NCMe)_4]^+ \quad (1)$$

constant throughout the entire temperature range; those for $[Cu(dmp)(NCMe)_x]^+$ progressively broaden and shift downfield on increasing temperature. Although the exact composition of $[Cu(dmp)(NCMe)_x]^+$ is not known, it is probable that a dynamic equilibrium exists between $[Cu(dmp)(NCMe)_2]^+$ and $[Cu(dmp)(NCMe)]^+$.

Room temperature ^1H NMR spectra of solutions of $[Cu(NCMe)_4][BF_4]$ **5** and dmp were recorded for constant **5** concentration (0.0485 mol dm^{-3}) and variable dmp concentration (0.00–0.0970 mol dm^{-3}). Careful integration of methyl signal intensities gave $[Cu(dmp)_2]^+$ and $[Cu(dmp)(NCMe)_x]^+$ concentrations and, by difference, $[Cu(NCMe)_4]^+$ concentration. These are plotted as a function of dmp concentration in Fig. 6. Both $[Cu(dmp)(NCMe)_x]^+$ and $[Cu(dmp)_2]^+$ are formed throughout the composition range. At low ratios $[Cu(dmp)(NCMe)_x]^+$ is the major product. As the ratio increases its concentration passes through a maximum (at an equimolar ratio) and it is ultimately replaced by $[Cu(dmp)_2]^+$ as the major product. An Arrhenius plot of the variable temperature data shows that the K_e value [3.9(6) at 298 K] is virtually temperature

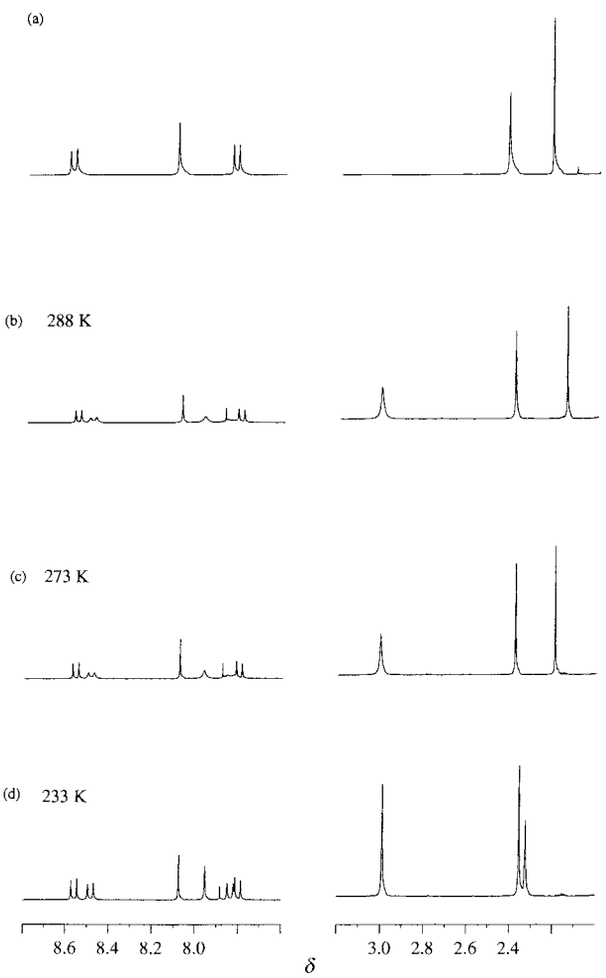

Fig. 5 Comparison of the variable temperature ^{1}H NMR spectra [288 (b), 273 (c), 233 K (d)] of [Cu(dmp)(NCMe)][BF_4] in deuteriated acetonitrile with the corresponding spectrum of [$Cu(dmp)_2$][BF_4] at 298 K (a).

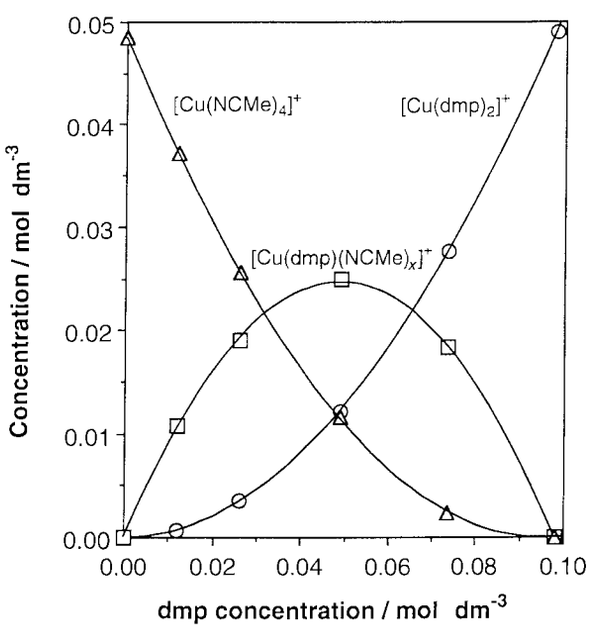

Fig. 6 Variation in the composition of acetonitrile solutions containing copper(I) tetrafluoroborate (0.0485 mol dm^{-3}) and 2,9-dimethyl-1,10-phenanthroline (0.00–0.0970 mol dm^{-3}) at 298 K.

independent, consistent with $\Delta H = -0.55$ kJ mol^{-1}, $\Delta S = 9.42$ J K^{-1} mol^{-1} and $\Delta G_{298} = -3.36$ kJ mol^{-1}.

The absence of co-ordinated cnge in solution suggests that the [Cu(dmp)(cnge)]$^+$ cation is formed during crystallisation and that its solid phase stability can be ascribed to π–π stacking interactions.

Conclusion

Stabilisation of three-co-ordinate copper(I) in [Cu(dmp)(nitrile)]$^+$ cations is due not to an intrinsic property of the molecular cation but to intermolecular π–π stacking interactions between co-ordinated dmp molecules. The parallel packing of the cations promotes planar co-ordination geometry in a similar fashion to the packing of the two-dimensional sheets constructed by N–H···F contacts in $CuBF_4$–cnge complexes.[17]

The lability of the [Cu(dmp)(nitrile)]$^+$ cations in MeCN solution has been established by ^{1}H NMR studies, the principal species being [$Cu(NCMe)_4$]$^+$, [$Cu(dmp)(nitrile)_x$]$^+$ ($x = 1$ or 2) and [$Cu(dmp)_2$]$^+$ cations. The formation of the [Cu(dmp)(nitrile)]$^+$ cation during crystallisation suggests that its solid phase stability may be attributed to intermolecular packing interactions.

The three complexes **1**, **2** and **3** can be envisaged to form part of a crystallographic interpretation of associative substitution of cnge by MeCN at trigonal planar copper(I). Starting with [Cu(dmp)(cnge)]$^+$ (as in **1**) and finishing with [Cu(dmp)(NCMe)]$^+$ (as in **3**), the mechanism initially involves a complex with a hydrogen-bonded MeCN molecule adjacent the copper(I) atom (as in **2**) and secondly a tetrahedral [Cu(dmp)(cnge)(NCMe)]$^+$ cation (as exemplified by the terminal copper atoms in **4**).[8]

Our success in generating mononuclear [Cu(dmp)(cnge)]$^+$ three-co-ordinate cations [Scheme 1(b)] suggests that our inability to prepare the dinuclear [{Cu(cnge)}$_2$(μ-L)]$^+$ (L = ppd, Meppd or Buppd) analogues [Scheme 1(a)] is due not to their intrinsic instabilities but to the greater relative stabilities of the alternative tetrahedrally co-ordinated products. For ppd and ppdMe the tetranuclear complexes [Cu_4(μ-L)$_4$]$^{4+}$ (L = ppd or Meppd) [Scheme 2(b)] are thermodynamic sinks. For ppdBu the steric demands of the *tert*-butyl groups not only prevent tetranuclear complex formation but also destroy the efficient packing of two-dimensional arrays and result in the trinuclear [Cu{(μ-ppdBu)Cu(cnge)(NCMe)}$_2$]$^{3+}$ cation [Scheme 2(a)].

Experimental

All reactions were carried out under a nitrogen atmosphere using standard Schlenk techniques unless otherwise noted. Nitrogen gas (Air Products) was dried by passage over molecular sieve (Linde 4A). All chemicals (Aldrich Chemical Company Ltd.) were reagent grade and, with the exception of cnge which was recrystallised from hot water, used as received. 2,9-Dimethyl-1,10-phenanthroline was used as the monohydrate (neocuproine hydrate). The solvents were dried before use by refluxing under dry nitrogen over the appropriate drying agent[24] and degassed using three freeze–thaw cycles.

The copper(I) starting material, [$Cu(NCMe)_4$][BF_4] **5**, was prepared either by addition of an excess of copper powder to the product of the reaction of copper gauze with $NOBF_4$ in MeCN[25] or by treatment of hydrated copper(II) tetrafluoroborate with copper powder in MeCN.[26]

The substituted 2-cyanoguanidines were obtained by reaction of dimethylammonium chloride with sodium dicyanamide (for cyano-*N*,*N*-dimethylguanidine)[27] or by treatment of pentane-2,4-dione with 2-cyanoguanidine in the presence of base (for 2-cyanoimino-4,6-dimethylpyrimidine).[28]

Elemental analyses and infrared spectra were consistent with the proposed product structures. Microanalytical data were obtained, using a PE 240B mass elemental analyzer, by Mr. T. J. Spencer of the University of Nottingham Chemistry Depart-

Table 4 Crystallographic data for complexes **1**–**3**

	1	**2**	**3**
Formula	$C_{16}H_{16}BCuF_4N_6 \cdot 0.5Et_2O$	$C_{16}H_{16}BCuF_4N_6 \cdot MeCN$	$C_{16}H_{15}BCuF_4N_3$
M	479.76	483.75	399.67
Crystal system	Orthorhombic	Monoclinic	Monoclinic
Space group	*Pbcn* (no. 60)	$P2_1/c$ (no. 14)	$P2_1/c$ (no. 14)
a/Å	16.547(5)	14.959(5)	11.848(16)
b/Å	19.404(12)	20.000(14)	19.296(3)
c/Å	13.657(4)	6.803(6)	7.5061(11)
β/°	—	92.35(5)	108.29(2)
Z	8	4	4
U/Å^3	4385(3)	2034(2)	1629(3)
μ(Mo-Kα)/mm^{-1}	1.05	1.13	1.39
Unique reflections	3875	3573	2849
R, R' (all data)	0.1335, 0.1411	0.0724, 0.0851	0.0383, 0.0390
(data with $I \geq 2\sigma(I)$)	0.0741, 0.0922	0.0574, 0.0717	0.0344, 0.0373

ment Analytical Services Group. The IR spectra were obtained in the range 4000–650 cm^{-1} using a Perkin-Elmer PE983G spectrometer as KBr pressed pellets, ^{1}H and ^{13}C NMR spectra on a Bruker DPX 300 spectrometer referenced to residual protio solvent (^{1}H) or solvent (^{13}C) resonances and reported relative to tetramethylsilane (δ 0).

Preparation of complexes

[Cu(dmp)(cnge)][BF$_4$]·0.5Et$_2$O 1. A solution of cnge (0.067 g, 0.80 mmol), dmp (0.166 g, 0.73 mmol) and freshly prepared complex **5** (0.25 g, 0.79 mmol) in CH_2Cl_2 (40 cm^3) was stirred for 16 h under a nitrogen atmosphere. Vapour phase diffusion of Et_2O gave a small number of yellow crystals (yield: 0.22 g, 0.46 mmol, 63%). Analysis: found (calculated for $C_{16}H_{16}BCuF_4N_6 \cdot 0.5Et_2O$) C 45.40 (45.05), H 4.65 (4.40), N 17.10 (17.50%). IR, $\tilde{\nu}$/cm^{-1} (cnge bands except when stated otherwise): 3428s, 3381m, 2206m, 2162s, 1641s, 1593m (dmp), 1567s (cnge or dmp), 1506m (cnge or dmp), 1381m (dmp), 1259m, 1070s (br) (BF_4^-), 930w, 851s (dmp), 725m (cnge or dmp), 667m, 548m (cnge or dmp).

[Cu(dmp)(cnge)][BF$_4$]·MeCN 2. A solution of cnge (0.067 g, 0.80 mmol), dmp (0.166 g, 0.73 mmol) and freshly prepared complex **5** (0.25 g, 0.79 mmol) in MeCN (40 cm^3) was stirred for 16 h under a nitrogen atmosphere. Vapour phase diffusion of Et_2O gave a small number of yellow crystals (yield: 0.15 g, 0.31 mmol, 42%). Analysis: found (calculated for $C_{16}H_{16}BCuF_4N_6 \cdot MeCN$) C 44.80 (44.70), H 4.15 (3.95), N 19.95 (20.25%). IR, $\tilde{\nu}$/cm^{-1} (cnge bands unless stated otherwise): 3440s, 3380m, 2206m, 2162s, 1645s, 1592m (dmp), 1565s (cnge or dmp), 1506m (cnge or dmp), 1382m (dmp), 1255m, 1070s (br) (BF_4^-), 929w, 852s (dmp), 721m (cnge or dmp), 669m, 550m (cnge or dmp).

[Cu(dmp)(NCMe)][BF$_4$] 3. Prepared as described previously.[18] Analysis: found (calculated for $C_{16}H_{15}BCuF_4N_3$) C 47.55 (48.10), H 3.65 (3.80), N 10.70 (10.50%). IR, $\tilde{\nu}$/cm^{-1} (dmp bands unless stated otherwise): 1592s, 1560m, 1496m, 1422m, 1381m, 1361m, 1142s, 1054s (br) (BF_4^-), 851s, 725m and 548m.

[Cu(dmp)(dmcnge)][BF$_4$] 7. A solution of dmcnge (0.16 g, 1.43 mmol), dmp (0.30 g, 1.33 mmol) and freshly prepared complex **5** (0.45 g, 1.43 mmol) in MeCN (40 cm^3) was stirred for 16 h under a nitrogen atmosphere. After reduction in volume, Et_2O was added to the red solution to yield a yellow precipitate. The solid was filtered off, dried and dissolved in the minimum volume of MeCN. Vapour phase diffusion of Et_2O gave a crop of fine yellow crystals (yield: 0.52 g, 1.10 mmol, 83%). Analysis: found (calculated for $C_{18}H_{20}BCuF_4N_6$) C 45.60 (45.95), H 4.10 (4.30), N 17.95 (17.85%). IR, $\tilde{\nu}$/cm^{-1} (dmcnge bands unless stated otherwise): 3396s, 3203m, 2163s, 1647s, 1593s (dmp), 1523s (dmcnge or dmp), 1424m, 1381m (dmp), 1310m, 1085s (br) (BF_4^-), 852s (dmp), 725m (dmcnge or dmp), 652m, 547m (dmp).

[Cu(dmp)(cidmp)][BF$_4$] 8. A solution of cidmp (0.21 g, 1.42 mmol), dmp (0.30 g, 1.33 mmol) and freshly prepared complex **5** (0.45 g, 1.43 mmol) in MeCN (60 cm^3) was stirred for 16 h under a nitrogen atmosphere. After filtration vapour phase diffusion of Et_2O gave a crop of small yellow crystals (yield: 0.47 g, 0.93 mmol, 70%). Analysis: found (calculated for $C_{21}H_{20}BCuF_4N_6$) C 49.25 (49.75), H 3.40 (3.95), N 16.20 (16.60%). IR, $\tilde{\nu}$/cm^{-1} (cidmp bands unless stated otherwise): 2856m, 2203s, 1646s, 1613s, 1593s (dmp), 1508m (dmp), 1444m (dmp), 1384m (dmp), 1314m, 1124m, 1085s (br) (BF_4^-), 852s (dmp) and 548m (dmp).

Crystallography

X-Rray diffraction data were collected at 220 (for complex **1**) or 150 K (for **2** and **3**) using a Stoe Stadi-4 four circle diffractometer with Oxford Cryosystems cryostat,[29] using scan type ω–θ (θ_{max} 25°). Empirical absorption corrections were applied for **1** and **3**.

The structures were solved by direct methods (SIR 92[30]) and refined by full matrix least squares (CRYSTALS[31]) on F^2 using all positive data. All hydrogen atoms in complexes **2** and **3** were found in Fourier difference syntheses; those in **1** were placed in calculated positions (X–H 1.00 Å). No disorder was observed. All non-hydrogen atoms were refined anisotropically. Hydrogen atoms in **2** and **3** were refined isotropically and those in **1** allowed to ride on their parent atoms in the calculated positions. Crystal data and details of the structure solutions are collated in Table 4. All structure diagrams were generated using the CAMERON computing package.[32]

CCDC reference number 186/1695.

See http//www.rsc.org/suppdata/dt/1999/4261/ for crystallographic files in .cif format.

Acknowledgements

We thank (i) the EPSRC for financial support (to D. J. Q), for PDRA support (to W.-S. L. and C. E. R) and for provision of a four-circle diffractometer and (ii) the University of Nottingham for financial support (to C. L. S.).

References

1 W. P. J. Gaykema, W. G. J. Hol, J. M. Verijken, N. M. Soeter, H. B. Bak and J. J. Beintena, *Nature* (*London*), 1984, **309**, 23; B. Linzen, N. M. Soeter, A. F. Riggs, H.-J. Schneider, W. Schartau, M. D. Moore, E. Yokata, P. Q. Behrens, H. Nakashima, T. Takagi, J. M. Nemeto, J. M. Verijken, H. B. Bak, J. J. Beintena and A. Volbeda, *Science* (*Washington*), 1985, **229**, 519; W. P. J. Gaykema, A. Volbeda

and W. G. J. Hol, *J. Mol. Biol.*, 1986, **187**, 255; B. Hazes, K. A. Magnus, C. Bonaventura, J. Bonaventura, Z. Dauter, K. H. Kalk and W. G. J. Hol, *Protein Sci.*, 1993, **2**, 597.
2 K. A. Magnus, H. Ton-That and J. E. Carpenter, in *Bioinorganic Chemistry of Copper*, eds. K. D. Karlin and Z. Tykeklár, Chapman and Hall, New York, 1993, p. 143; K. A. Magnus, B. Hazes, C. Bonaventura, J. Bonaventura and W. G. J. Hol, *Proteins: Struct., Funct., Genet.*, 1994, **19**, 302.
3 A. S. Batsanov, M. J. Begley, P. Hubberstey and J. Stroud, *J. Chem. Soc., Dalton Trans.*, 1996, 1947.
4 M. J. Begley, P. Hubberstey and P. H. Walton, *J. Chem. Soc., Dalton Trans.*, 1995, 957; *J. Chem. Soc., Chem. Commun*, 1989, 502.
5 M. J. Begley, O. Eisenstein, P. Hubberstey, S. Jackson, C. E. Russell and P. H. Walton, *J. Chem. Soc., Dalton Trans.*, 1994, 1935.
6 M. J. Begley, P. Hubberstey, C. E. Russell and P. H. Walton, *J. Chem. Soc., Dalton Trans.*, 1994, 2483.
7 M. Munakata, M. Maekawa, S. Kitagawa, S. Matsuyama and H. Masuda, *Inorg. Chem.*, 1989, **28**, 4300.
8 P. Hubberstey and C. E. Russell, *J. Chem. Soc., Chem. Commun*, 1995, 959.
9 P. Hubberstey and C. E. Russell, unpublished results.
10 C. E. Holloway and M. Melnik, *Rev. Inorg. Chem.*, 1995, **15**, 147.
11 T. A. Annan, R. Kumar and D. G. Tuck, *Inorg. Chem.*, 1990, **29**, 2475; M. Hakansson, S. Jagner, E. Clot and O. Eisenstein, *Inorg. Chem.*, 1992, **31**, 5389; J. F. Reidl, I. El-Idrissi Rachidi, Y. Jean and M. Pellissier, *New. J. Chem.*, 1991, **15**, 239; J. K. Burdett and O. Eisenstein, *Inorg. Chem.*, 1992, **31**, 1758.
12 A. Baiada, F. H. Jardine, R. D. Willett and K. Emerson, *Inorg. Chem.*, 1991, **30**, 1365.
13 K. D. Karlin, Y. Gultneh, J. P. Hutchinson and J. Zubieta, *J. Am. Chem. Soc.*, 1982, **104**, 5240; T. M. Sorrell and M. R. Malachowki, *Inorg. Chem.*, 1983, **22**, 1883; J. V. Dagdigian, V. McKee and C. A. Reed, *Inorg. Chem.*, 1982, **21**, 1332.
14 S. M. Nelson, F. Esho, A. Lavery and M. G. B. Drew, *J. Am. Chem. Soc.*, 1983, **105**, 5693.
15 G. A. Bowmaker, G. R. Clark, D. A. Rogers, A. Camus and N. Marsich, *J. Chem. Soc., Dalton Trans.*, 1984, 37.
16 C. Kappenstein and R. P. Hugel, *Inorg. Chem.*, 1978, **17**, 1945; C. Kappenstein and R. P. Hugel, *Inorg. Chem.*, 1977, **16**, 250.
17 A. S. Batsanov, M. J. Begley, M. W. George, P. Hubberstey, M. Munakata, C. E. Russell and P. H. Walton, preceding paper.
18 A. J. Blake, S. J. Hill, P. Hubberstey and W.-S. Li, *J. Chem. Soc., Dalton Trans.*, 1998, 909.
19 I. Csoregh, P. Kierkegaard and R. Norrestam, *Acta Crystallogr., Sect. B*, 1975, **31**, 314.
20 W. J. Jones and W. J. Orville-Thomas, *Trans. Faraday Soc.*, 1959, **55**, 193.
21 M. J. Begley, P. Hubberstey and J. Stroud, *J. Chem. Soc., Dalton Trans.*, 1996, 2323.
22 A. S. Batsanov, P. Hubberstey, C. E. Russell and P. H. Walton, *J. Chem. Soc., Dalton Trans.*, 1997, 2667.
23 J. Dai, M. Yamamoto, T. Kuroda-Sowa, M. Maekawa, Y. Suenaga and M. Munakata, *Inorg. Chem.*, 1997, **36**, 2688.
24 D. D. Perrin and W. L. F. Armarego, *Purification of Laboratory Chemicals*, Pergamon, Oxford, 3rd edn., 1988.
25 B. J. Hathaway, D. G. Holah and J. P. Postlethwaite, *J. Chem. Soc.*, 1961, 3215.
26 G. J. Kubas, *Inorg. Synth.*, 1979, **19**, 90.
27 F. H. S. Curd, J. A. Hendry, T. S. Kenny, A. G. Murray and F. Rose, *J. Chem. Soc.*, 1948, 1630.
28 W. J. Hale and F. C. Vibrans, *J. Am. Chem. Soc.*, 1918, **40**, 1046.
29 J. Cosier and A. M. Glazer, *J. Appl. Crystallogr.*, 1986, **19**, 105.
30 A. Altomare, G. Cascarano, G. Giacovazzo, A. Guagliardi, M. C. Burla, G. Polidori and M. Camalli, *J. Appl. Crystallogr.*, 1994, **27**, 435.
31 D. J. Watkin, C. K. Prout, R. J. Carruthers and P. Betheridge, CRYSTALS, Issue 10, Chemical Crystallography Laboratory, University of Oxford, 1996.
32 D. J. Watkin, C. K. Prout and L. J. Pearce, CAMERON, Chemical Crystallography Laboratory, University of Oxford, 1996.

Paper 9/06781G